

# Differential correction method applied to measurement of the FAST reflector

Xin-Yi Li<sup>1,2</sup>, Li-Chun Zhu<sup>1,†</sup>, Jin-Wen Hu<sup>1</sup> and Zhi-Heng Li<sup>1</sup>

<sup>1</sup> National Astronomical Observatories, Chinese Academy of Sciences, Beijing 100012, China;  
*lixinyi10@mails.ucas.ac.cn; lczhu@bao.ac.cn*

<sup>2</sup> University of Chinese Academy of Sciences, Beijing 100049, China

Received 2016 March 1; accepted 2016 March 22

**Abstract** The Five-hundred-meter Aperture Spherical radio Telescope (FAST) adopts an active deformable main reflector which is composed of 4450 triangular panels. During an observation, the illuminated area of the reflector is deformed into a 300-m diameter paraboloid and directed toward a source. To achieve accurate control of the reflector shape, positions of 2226 nodes distributed around the entire reflector must be measured with sufficient precision within a limited time, which is a challenging task because of the large scale. Measurement of the FAST reflector makes use of stations and node targets. However, in this case the effect of the atmosphere on measurement accuracy is a significant issue. This paper investigates a differential correction method for total stations measurement of the FAST reflector. A multi-benchmark differential correction method, including a scheme for benchmark selection and weight assignment, is proposed. On-site evaluation experiments show there is an improvement of 70%–80% in measurement accuracy compared with the uncorrected measurement, verifying the effectiveness of the proposed method.

**Key words:** telescopes — FAST — measurement — differential correction

## 1 INTRODUCTION

The Five-hundred-meter Aperture Spherical radio Telescope (FAST) is an Arecibo-type spherical telescope. The active main reflector with a diameter of 500 m directly corrects spherical aberration (Nan 2008). It consists of a 500-meter diameter ring beam, a main cable mesh composed of 6670 strands of steel cables, 2226 down-tied cables connecting the cable mesh to the winches on the ground, and 4450 triangular panels mounted on the cable mesh (Nan 2006). Hydraulic actuators are installed under the down-tied cables. They can adjust their own lengths in order to control the shape of the cable mesh in real time. When the telescope is observing target sources, the illuminated area of the reflector will be deformed into a 300 m diameter paraboloid pointed toward the source direction to collect radio signals and reflect them onto the feeds of receivers in the feed cabin (Hu et al. 2013). The structure of the main reflector is shown in Figure 1.

The FAST reflector control system uses nodes which are intersections of the cable mesh and down-tied cables as control points. The reflector's measurement system uses high-precision prisms which are installed on nodes as measurement targets. The measurement system has two primary working modes: calibration mode and observing mode. In calibration mode, the goal is measuring all the 2226 targets in 90 min, for which the required precision is

1.5 mm; in observing mode, the goal is measuring  $\sim 700$  targets in the corresponding paraboloidal area in 10 min, for which the required precision is 2 mm.

The difficulties in reflector measurement are:

- (1) The reflector is dynamic and deformable;
- (2) Long distance measurement in the field environment;
- (3) Having a relative accuracy in distance of about 1:125 000.

A measurement procedure that can overcome the above mentioned difficulties is very challenging for us.

## 2 MEASUREMENT SYSTEM OF REFLECTOR

The measurement system of the active reflector mainly consists of 10 total stations, 2226 targets and 23 foundation piers. Targets are fixed on all the nodes, and 10 total stations are installed on the five central foundation piers. Other piers are used as measurement differential correction benchmarks. When the telescope is observing, total stations scan the  $\sim 700$  targets in the required paraboloid in a measurement cycle.

### 2.1 Foundation Piers

During the construction of FAST, 23 foundation piers were built, named JD1 to JD23 (see Fig. 2). The piers are arranged in three loops. We call them the inner loop, the

† Corresponding author.

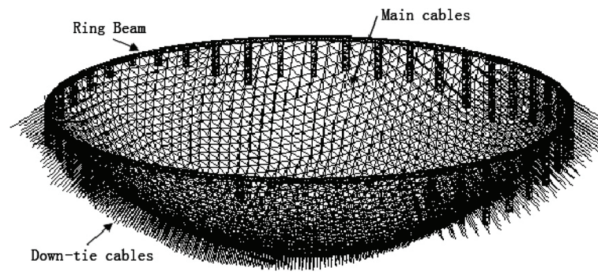


Fig. 1 Structure of the main reflector.

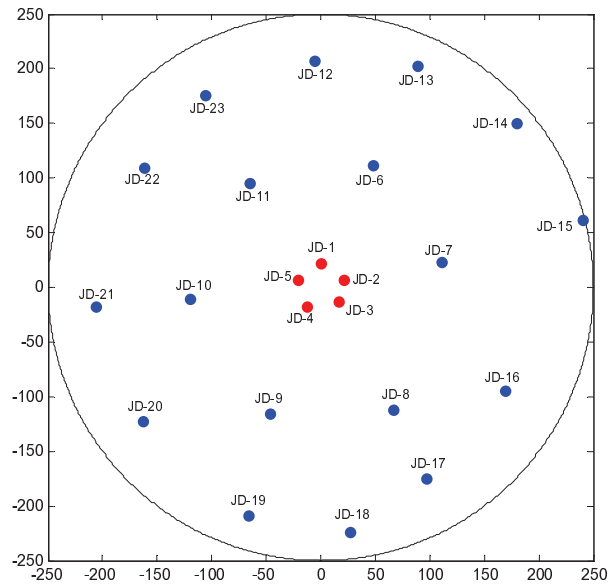


Fig. 2 Distribution of foundation piers.

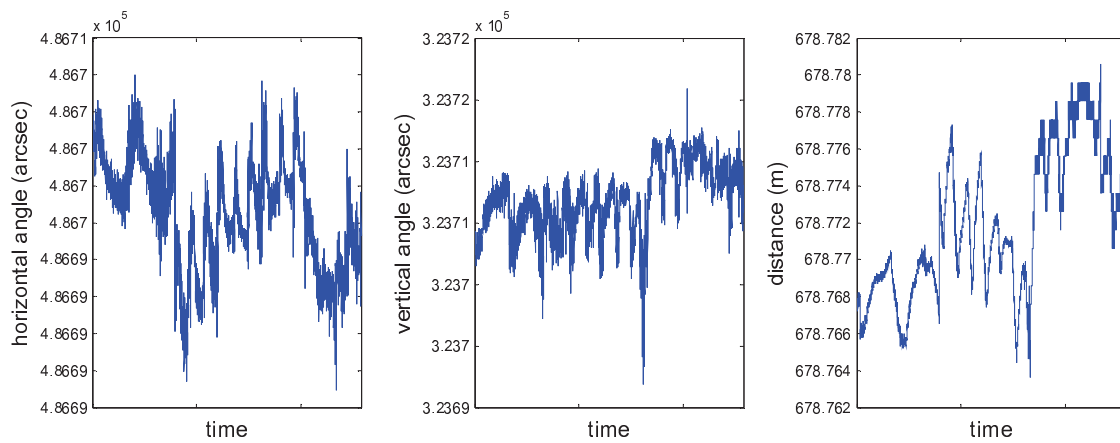


Fig. 3 Angles and distance monitoring curves.

middle loop and the outer loop. The reflector measurement system is designed to use ten total stations which will be fixed on the five piers in the inner loop. Two total stations will be installed on each pier. On the top of each pier, there are three forced centering plates which can support three devices working simultaneously.

## 2.2 Measuring Device

Total stations have the advantages of being suitable for fieldwork, high reliability, high measurement accuracy, and programmability. They can measure multiple targets with high precision automatically. When the measure-

ment system is working, ten total stations will apply the Automatic Target Recognition (ATR) model (Zeiske 2000) simultaneously.

### 2.3 Targets

2226 high-precision prism targets are fixed on the nodes of the cable mesh. They are facing the intersection of total station levels and central vertical axis of the reflector.

## 3 NECESSITY OF DIFFERENTIAL CORRECTION METHOD

The effect of the environment on accuracy of long-distance field measurement is still a problem (Ogundare 2015). We have done an experiment on intermittent monitoring for a month at the FAST site to investigate the effect of the environment. The monitored target's angles and distance curves are shown in Figure 3.

When conducting the monitoring, measurement data show large fluctuations. This demonstrates the strong influence of the environment. The difference in distance reaches up to 17 mm. The distance error caused by atmospheric refraction can be effectively eliminated by several atmospheric correction methods (e.g. PIF, RCS and COST) which are commonly used in measurement projects (Bertacchini et al. 2011; Mahiny & Turner 2007).

Besides distance, atmospheric refraction also introduces error to angles. In Figure 3, the difference in horizontal angle and vertical angle respectively reaches 17.1'' and 24.1''. This can lead to an error of up to 28.62 mm in angular deflection on a scale of 200 m. However, at present there is no appropriate empirical formula to correct this error.

Based solely on this fact, in the FAST reflector measurement system, angle measurement error is the main problem which needs to be overcome. The differential correction method is usually used to correct 3-dimensional positions in GPS measurements (Rempel & Rodgers 1997). Inspired by this, we propose a multi-benchmark differential correction method applied to FAST to solve the problem. Through experiments and calculations, this method can reduce the angle measurement error caused by atmospheric disturbance. The improvement in a target's measurement coordinate precision can reach up to 70%–80%.

## 4 DIFFERENTIAL CORRECTION METHOD

Through a 1-year monitoring program, the piers are shown to be stable and reliable in that their deformation is less than 1 mm. On the other hand, the piers have approximately the same atmospheric conditions as measuring targets. Therefore, the piers can be used in the FAST reflector measurement system as differential benchmark stations.

### 4.1 General Algorithm

We define a measured true value  $B$  of the differential benchmark beforehand and continuously monitor the real-

time measured value of this benchmark  $BR$  and of all the targets  $TR$ . By calculating the proportional difference in a benchmark's true value  $B$  and real-time value  $BR$ , we can get the correction coefficient of targets.

The differential correction coefficient is

$$d_o = \frac{BR - B}{BR} = 1 - \frac{B}{BR}. \quad (1)$$

Hence the target's correction value is

$$\begin{aligned} TB_o &= TR - TR \cdot d_o = TR \cdot (1 - d_o) \\ &= \frac{TR \cdot B}{BR}. \end{aligned} \quad (2)$$

A single target's Root Mean Square Error (RMSE) under repeated measurements is used as a criterion for evaluation of precision in this paper. From Equation (2) it is found that RMSE will equal 0 when  $TR/BR = 1$ . That is, the closer the benchmark and target's dynamic measurement curves are, the better the effect of differential correction is. Therefore, similar atmospheric conditions between benchmark and targets are preferred.

### 4.2 Multi-Benchmark Algorithm

Based on the above-mentioned considerations, we propose a multi-benchmark algorithm.

Consider the equal distribution of multiple benchmarks. The differential correction coefficient will be

$$d_b = \frac{1}{N} \sum_{i=1}^N \frac{BR_i - B_i}{BR_i}, \quad (3)$$

where  $B_i$  is each benchmark's true value,  $i = 1, 2, 3, \dots, N$ .  $BR_i$  is each benchmark's measured real-time value,  $i = 1, 2, 3, \dots, N$ .

The correction that is applied to the target is

$$\begin{aligned} TB_b &= TR - TR \cdot d_b = TR \cdot (1 - d_b) \\ &= TR \cdot \left( 1 - \frac{1}{N} \sum_{i=1}^N \frac{BR_i - B_i}{BR_i} \right), \end{aligned} \quad (4)$$

where  $TR$  is the target's real-time measured value.

### 4.3 Weight Assignments in the Multi-Benchmark Algorithm

A weighting factor is assigned to each differential correction. The differential correction coefficient becomes

$$d_w = \sum_{i=1}^N \frac{BR_i - B_i}{BR_i} \cdot \rho_i, \quad (5)$$

where  $\rho_i$  is each benchmark station's weight coefficient. The sum of the coefficients is 1.

The target's correction value is

$$\begin{aligned} TB_w &= TR - TR \cdot d_w = TR \cdot (1 - d_w) \\ &= TR \cdot \left( 1 - \sum_{i=1}^N \frac{BR_i - B_i}{BR_i} \cdot \rho_i \right). \end{aligned} \quad (6)$$

The specific number and coefficient of piers in the process of reflector measurement for FAST will be determined by experiments.

#### 4.4 Processing Horizontal Angle Data

The measurement data uploaded by all of the stations include three separate observations: distance, horizontal angle and vertical angle. Distance and vertical angle data can be processed by the above proportional difference method. However, the horizontal angle is not suitable for it. We use an offset correction method to deal with the horizontal angle data.

For a single benchmark, a measured true value  $BH$  of the benchmark's horizontal angle is collected beforehand. At any moment, we get the real-time measured horizontal angle of this benchmark  $BRH$  and of all the targets  $TRH$ . The correction coefficient is

$$c_o = BRH - BH. \quad (7)$$

Hence the target's corrected value is

$$TBH_o = TRH - c_o = TRH - BRH + BH. \quad (8)$$

For weighted multiple benchmarks, the correction coefficient becomes

$$c_w = \sum_{i=1}^N (BRH_i - BH_i) \cdot \rho_i, \quad (9)$$

where  $BH_i$  is each benchmark's measured true value of horizontal angle,  $i = 1, 2, 3, \dots, N$ .  $BRH_i$  is each benchmark's measured real-time horizontal angle,  $i = 1, 2, 3, \dots, N$ .  $\rho_i$  is each benchmark station's weight coefficient. The sum of the coefficients is 1.

The target's correction value becomes

$$\begin{aligned} TBH_w &= TRH - c_w \\ &= TRH - \sum_{i=1}^N (BRH_i - BH_i) \cdot \rho_i. \end{aligned} \quad (10)$$

## 5 EXPERIMENTAL RESULTS

At the FAST project site, we have performed two relevant experiments to verify the above-mentioned algorithms. In the experiments, we use the mean value as the true value.

### 5.1 Basic Experiment

The first experiment lasted for 47h over two successive days. In this experiment, one total station was set on pier JD4 as the survey station. Seven targets were set on JD6, JD7, JD9, JD10, JD18, JD20 and JD21 respectively (see Fig. 4). The total station used the ATR mode to measure the targets circularly and repeatedly measured each target five times. The cycle time was about 200 s.

#### 5.1.1 Analysis of the basic differential correction method

We defined one of the targets as a differential benchmark and calculated the correction values for the remaining six targets. Distance and vertical angle come from Equations (1) and (2); horizontal angle comes from Equations (7) and (8).

Calculating respectively each pier as a differential benchmark, the variation of other targets' RMSE on distance, vertical angle and horizontal angle is shown in Figure 5. Measurement accuracy of these three observations has been improved significantly. The accuracy of distance, vertical angle and horizontal angle respectively improves by 57%, 38% and 58% on average. Increasing the number of benchmarks can increase the differential correction stability, especially for vertical angles.

After observing one of the targets (for instance JD10), the variation curves of its rectangular coordinates  $X$ ,  $Y$  and  $Z$  before and after the above correction are shown in Figure 6. The results demonstrate that the rectangular coordinate curves have leveled off significantly when these correction methods are applied.

#### 5.1.2 Availability of multi-benchmark

By using Equations (3) and (4), we can calculate the RMSE of all the targets by combinations of different benchmarks. For instance, the result of JD10 is shown in Table 1.

The results demonstrate that the multi-benchmark method is applicable to this study and can further improve the precision of differential correction. The increase in accuracy can be from 56% to 73% compared with the single benchmark method.

## 5.2 Multi-Benchmark Differential Correction Experiment

In order to further explore the multi-benchmark differential correction method and its application to the FAST project, we ran an experiment over 10 d, during which the same measurement model was applied over 53 h. One total station was set on pier JD4 as the survey station. Nine targets were set on JD7, JD8, JD9, JD10, JD17, JD18, JD19, JD20 and JD21 respectively (see Fig. 7).

#### 5.2.1 Selecting the number of benchmarks

Comparing the correction RMSE for five targets with a rectangular coordinate system for various numbers of benchmarks according to Equations (5), (6), (9) and (10), the effect of the different benchmark numbers is shown in Figure 8.

Considering accuracy and efficiency, we choose three-benchmark schemes in the FAST reflector's measurement system.

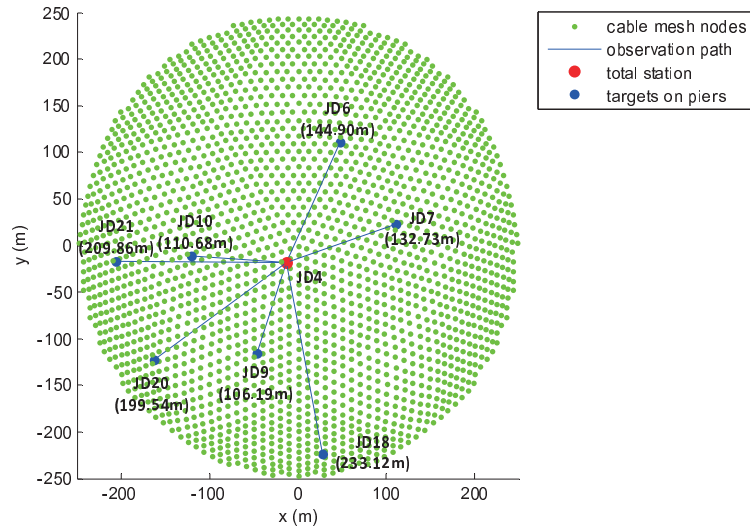


Fig. 4 Basic experimental settings.

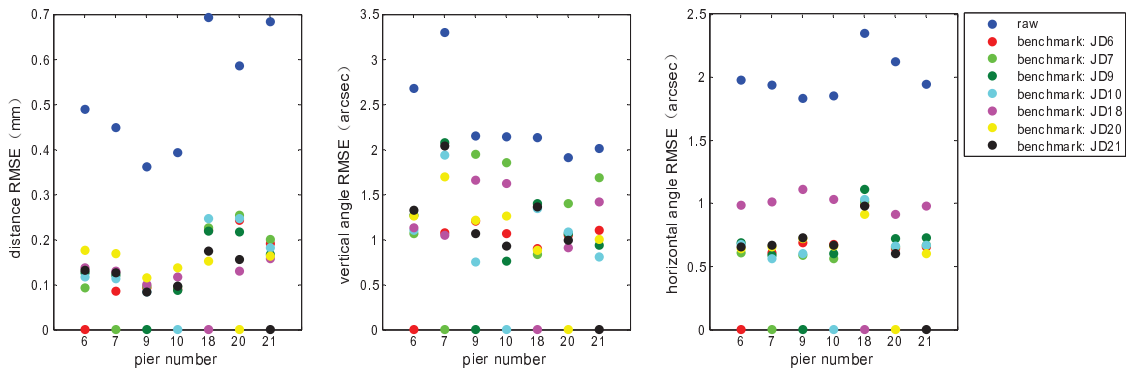


Fig. 5 Variation of RMSE with distance, vertical angle and horizontal angle.

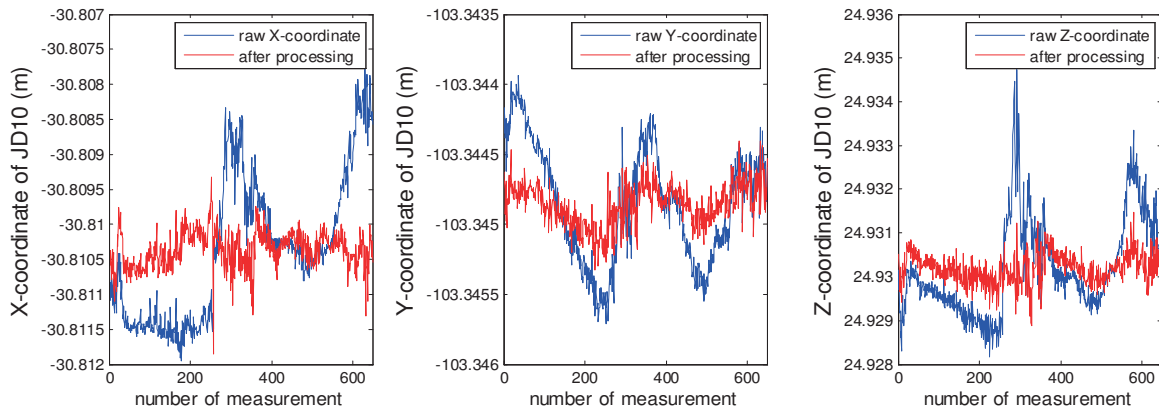


Fig. 6 Variation curves of JD10's rectangular coordinates.

Table 1 JD10's Correction RMSE by Different Benchmark Combinations

Benchmark combination	Raw	JD6	JD6 JD9	JD6 JD9 JD21
RMSE (mm)	0.90	0.39	0.27	0.25

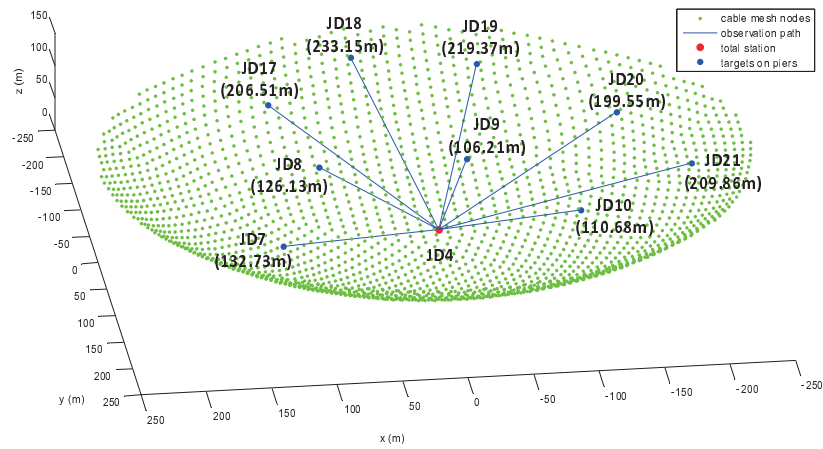


Fig. 7 Multi-benchmark experiment settings.

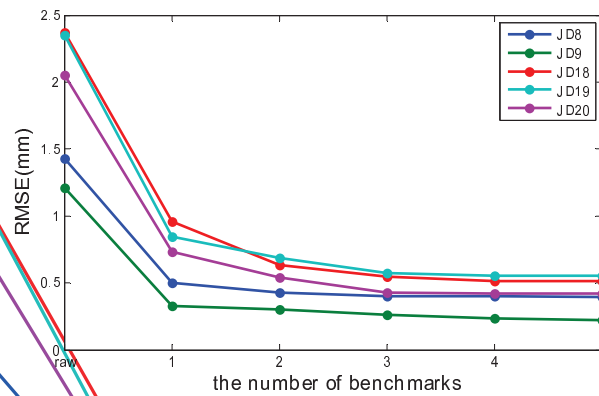


Fig. 8 Effect of the number of benchmarks on precision.

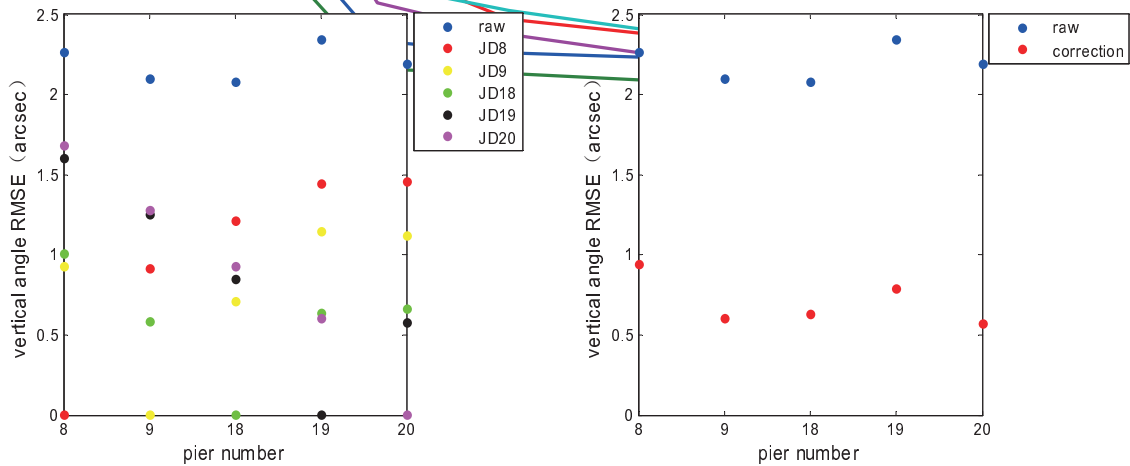


Fig. 9 Comparison of general method and multi-benchmark method on vertical angle error.

5.2.2 Multi-benchmark selection and their weight assignments

As Section 4.1 mentioned, similar atmospheric conditions between benchmark and targets are preferred, as was demonstrated when analyzing the experimental data. The most effective benchmark was closest to the target and had

approximately the same height as the target. So, we choose the two adjacent piers beside the target in the same loop as two benchmarks named P1 and P2. A pier which is located in the other loop is chosen as the third benchmark P3. By calculating and considering a practical design, we choose the pier which has the closest horizontal angle to a target as P3.

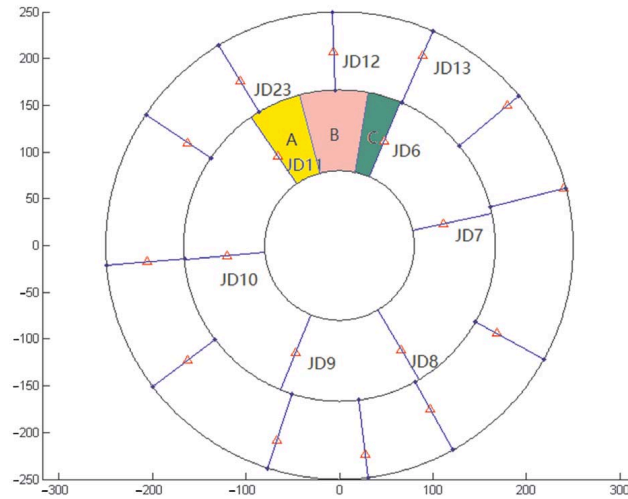


Fig. 10 Distribution map of nodes on circles.

Table 2 Results by Using Multi-benchmark Weight Assignments

Target	Raw	Correction	Accuracy improved	Benchmarks		
	RMSE (mm)	RMSE (mm)		(40%	40%	20%)
JD8	1.43	0.39	73%	JD7	JD9	JD17
JD9	1.21	0.24	80%	JD8	JD10	JD19
JD18	2.37	0.52	78%	JD17	JD19	JD8
JD19	2.35	0.56	76%	JD18	JD20	JD9
JD20	2.05	0.41	80%	JD19	JD21	JD9

A great number of calculation results have shown that the optimized weight assignments of P1, P2 and P3 are 0.4:0.4:0.2. The correction accuracy from the experiment by using these weight assignments is shown in Table 2.

After using this multi-benchmark selection and weight assignment method, the increase in accuracy can reach up to 78% on average.

As Section 5.1.1 mentioned, the multi-benchmark approach could significantly increase the stability of differential correction when applied to the vertical angle. The comparison of using the general single benchmark method with the multi-benchmark method from Section 5.2.2 when applied to processing vertical angle data is shown in Figure 9. The multi-benchmark approach can systematically improve precision. Not only is precision higher, but also the stability has been enhanced.

## 6 APPLICATION TO MEASUREMENT OF THE FAST REFLECTOR

Through the preceding analysis, we have designed a scheme that is applicable to measuring the FAST reflector.

We divide all the target nodes into three sections: inner ring, middle ring and outer ring. According to the positions of the piers, we set the boundary between the outer ring and middle ring as a circle where the radius to the center of the reflector is 167 m. We also set the boundary between the

middle ring and inner ring as the circle where the radius to the center of the reflector is 80 m. The distribution map is shown in Figure 10.

For targets in the inner ring, the measurement data do not need differential correction processing. For targets in the middle ring and outer ring, we choose the nearest two piers in the same ring as 40% weight differential correction benchmarks, and choose the closest horizontal angle pier in the other loop as the 20% weight differential correction benchmark.

For example, targets in areas A, B and C can all use JD11 and JD6 as 40% weight differential correction benchmarks. However, they use respectively JD23, JD12 and JD13 as the 20% weight differential correction benchmarks.

## 7 CONCLUSIONS

As confirmed by experiments, the differential correction method is effective. In addition, the multi-benchmark method presented in this paper can increase stability and reliability of measurement data. Moreover, it has been applied to the FAST reflector measurement system with good results.

**Acknowledgements** This work was supported by the Project Research of Adaptive Modeling and Control Strategy in the FAST Active Reflector of the National

Natural Science Foundation of China (Grant No. 11273001) and the Key Laboratory of Radio Astronomy, Chinese Academy of Sciences.

## References

- Bertacchini, E., Cappa, A., Castagnetti, C., & Corsini, A. 2011, *STA*, 15, 67
- Hu, J., Nan, R., Zhu, L., & Li, X. 2013, *Measurement Science and Technology*, 24, 095006
- Mahiny, A. S., & Turner, B. J. 2007, *Photogrammetric Engineering & Remote Sensing*, 73, 361
- Nan, R. 2006, *Science in China: Physics, Mechanics and Astronomy*, 49, 129
- Nan, R. 2008, in *SPIE Astronomical Telescopes+ Instrumentation*, International Society for Optics and Photonics, 70121E
- Ogundare, J. O. 2015, *Precision Surveying: The Principles and Geomatics Practice* (John Wiley & Sons)
- Rempel, R. S., & Rodgers, A. R. 1997, *The Journal of Wildlife Management*, 61, 525
- Zeiske, K. 2000, *Surveying Made Easy*, in *Leica Geosystems AG*, Heerbrugg, Switzerland, 35